Uncertainty factors in wind hazard analysis for tornado probabilistic risk assessment

Kota Fujiwara[a*], Daisuke Nohara[a], Yuzuru Eguchi[a], Hiromaru Hirakuchi[a], Yasuo Hattori[a]
[a]Central Research Institute of Electric Power Industry, Abiko, Japan

Abstract: The advancement of hazard assessment technologies for nuclear power plants (NPPs) is crucial towards the achievement of Level 1 tornado probabilistic risk assessment (PRA). A best estimate hazard analysis should be pursued using state-of-the-art methodology using the latest databases, while considering local tornado characteristics, is highly regarded. This study aims to establish an uncertainty method concerning wind hazard analysis for tornado PRA, applicable for NPPs in Japan. Following a concise overview of tornado wind hazard analysis, potential uncertainty sources will be deliberated based on existing studies. Notably, there is a lack of knowledge regarding uncertainty analysis for tornado width and length information. Based on this examination, our original tornado hazard analysis model will be proposed, alongside suggestions of methodologies for considering standard error analysis regarding tornado width and length as damage area uncertainty. Finally, a comparative case study was conducted for hazard curves and confidence intervals calculated under different methodologies. The Monte Carlo simulation-based method was determined to have the largest confidence interval, while also being the most appropriate among the compared methods.
Keywords: Tornado wind hazard curve, High wind PRA, Tornado.

1. INTRODUCTION

A tornado is a violent weather event that produces a column of rotating air, followed by intense upward flow [1]. The severity of tornadoes is typically quantified using tornado intensity scales, such as the Fujita scale (F-scale), which are based on the damage indicators observed after the tornadoes have passed. In Japan, tornadoes frequently occur proximity at the coastal regions [2], where several nuclear power plants (NPPs) are situated. Although Japan is not known as a tornado prone country, this geographic characteristic requires the implementation of robust safety measures in NPPs to withstand potential hazards by tornadoes.

There are some records that a tornado has resulted in the disruption of NPP operations, leading to loss of external power and/or damage to components [3]. To prevent catastrophic failure, it is essential for NPP systems structure and components (SSCs) be capable of withstanding the wind speeds associated with tornadoes. The procedure to determine the design basis tornado wind speed varies by regulatory authority. For actual guidelines, refer to documents such as the United States Nuclear Regulatory Commission (USNRC) Regulatory Guide 1.76 [4] or the assessment guide for tornado effect on NPPs JNES-RE–2013-9009 [5]. These guidelines require the calculation of the annual exceedance probability of wind speeds. This information can be obtained by collecting data from relevant databases, correcting for biases, and conducting data analysis. Statistical information from of tornadoes can then be applied to a wind hazard analysis. Guidelines for these procedures are written in Electric Power Research Institute (EPRI) Reports NP-2005 [6], NP-768/769 [7,8], or NUREG/CR-4461 ver2 [9].

To conduct a best estimate plus uncertainty hazard analysis, it is necessary to evaluate the hazard curve using a model that matches the tornado characteristics of Japan, while addressing the epistemic and aleatory uncertainty sources. The list of such sources varies between guidelines, so a comprehensive review should be conducted. In this article, potential uncertainty sources will be discussed based on existing studies in section 2. Based on the review, it was shown that there is a lack of knowledge regarding uncertainty analysis for tornado width and length information. Based on such examination, our original tornado hazard analysis model will be proposed in section 3, alongside suggestions of methodologies for considering uncertainty regarding tornado width and length as a measure of damage area uncertainty. Finally, in section 4, a comparative case study on the suggested methodologies will be conducted.

2. TORNADO WIND HAZARD ANALYSIS

2.1. Exceedance probability of wind speed

The aim of a wind hazard analysis is to estimate the annual return period of wind speed at a specific site. The ASME/ANS RA-Sb-2009 standard [10] requires the use of the state-of-art methodology and the most recent databases on tornadoes, and to propagate uncertainties in the model and parameter values to obtain a hazard curve. To achieve this, one should choose an appropriate data source, specify a characteristic region, correct/adjust the data, and conduct a probabilistic wind hazard assessment.

Wind hazard (P_{v0}) can be obtained by multiplying the tornado strike probability (P) by the conditional probability of tornado wind speed surpassing a specific wind speed (P ($u \geq u_0 | s$)). P is calculated by dividing the expected damage area by tornadoes (E (DA)) with the total area of interest (A_R), and then multiplying by the annual occurrence of events. P ($u \geq u_0 | s$) is derived from track observation data of tornadoes [11, 12]. The expected area of a tornado with width (W) and length (L), characteristic target size (D) is illustrated in Figure 1. The area can be split into Term1: the area of the tornado path ($W \times L$) corresponding to the probability of expect tornado path area in a given area (point strike probability), Term2: the tornado area intersecting the defined target ($L \times D$) (life-line probability), Term3 and 4: the areas at both ends ($W \times D$) and ($D \times D$). Generally speaking, for small structures, tornado length far exceeds the width ($L >> W$) and the target size is small, Term 1 is dominant. In case of a large target such as an NPP ($D \approx W$), Term 2 will may also become significant. NUREG/CR-4461 Revision 2 [9] considers both point strike and life-line probability. EPRI Report NP-2005 considers terms 1–4 [6].

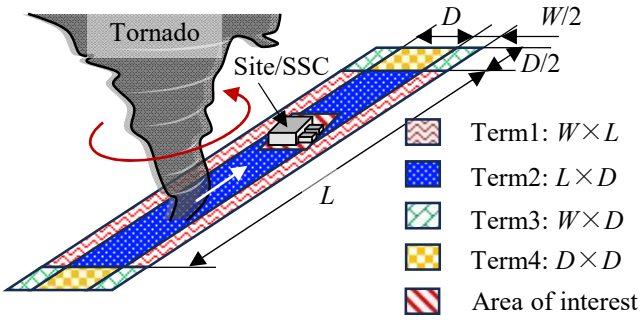

Figure 1. Definition of Expected Area

2.2. Uncertainty factors

Tornadoes are a local phenomenon and difficult to observe directly. Usually, the intensity and size of tornadoes are often inferred by examining the aftermath of tornado damage. This indirect approach introduces uncertainty in tornado records. In this section, the potential uncertainty sources will be discussed by classifying them into data source origin, wind speed assignment origin, occurrence rate origin, and path length/width origin.

Regarding data sources, tornado reports are known to have a changing trend, often an increase over time, based on the recorded period. This does not directly imply that tornadoes are increasing due to climatology, but due to various factors such as minor changes in reporting protocols, update in measurement systems [13], increasing population density [14] and feedback from the community. This results in epistemic uncertainty due to changes in data recording methods. For example, Agee and Childs (2014) [13] have used the data from 1950–2012, concluded that there is an inhomogeneity of F0/EF0 tornadoes between 1950–1952, 1953–1991, 1991~. NUREG/CR-4461 Rev.2 [9] compared the annual counts of F0 and F1–F5 tornadoes from 1950–2003. They concluded that the increase of annual counts was mainly attributed to F0 tornadoes but did not consider such increase in the analysis as its effect on total damage area was negligible. EPRI Report NP-2005 [6] investigated the total numbers of tornadoes from 1950–1978 and investigated the 8-, 9-, 10- and 29-year average. The data with maximum mean was adopted as annual mean. Intensity scale misclassification is another source of uncertainty. Two primary sources; direct classification error and random encounter error are defined. The direct classification error is related to judgement errors on the tornado intensity classification. EPRI Report NP-2005 [6] has defined such sources by assuming normal distribution for each count, with mean as the midpoint of the wind speed interval, and standard deviation to cover the range ±50 % increase in force.

Later in NUREG/CR-2944 [11], the standard deviation was defined as equivalent to 1/3 times the median velocity of adjacent wind speed class. These are purely aleatory uncertainties. The random encounter error is related to the percentage whether the tornadoes pass through a certain damage indicator when it has maximum intensity. Tornados do not maintain their maximum intensity throughout their path length. When damage indicators are limited or missed when reaching maximum intensity, it may lead to under classification. EPRI Report NP-2005 [6] treated such error by defining tornado damage area encounter probabilities, then multiplied with expected area of F_i damage in a F_k storm, derived from the path length intensity from observation data. NUREG/CR-2944 [11] used a simpler model by simply defining that the conditional probability by classifying a tornado in an adjacent wind speed category with 10 percent cascading error. The expected area could be a source of epistemic uncertainty as some observation data are available [11,12], while the encounter probability is a pure aleatory uncertainty source.

Regarding wind speed assignment, the F-scale has a discrete range of wind speed. The conversion from recorded F-scale to wind speed is crucial for defining a hazard curve. Typically, statistics within an F-scale converge to midpoint of the wind speed interval [9]. However, some experts argued that the original F-scale wind speeds are too high, especially for high wind speeds [7,8]. Adjusted wind speeds such as F' scale, the velocity discussed in the Texas Tech. University forum, has been proposed. Based on recent investigations and the new Degree of Damage approach, the EF-scale introduces a modified wind speed classification, followed by an ability to specify the corresponding wind speed to each specific event. The Japanese Enhanced F-scale [15] also provides a similar function. Such wind speed categorization should be considered as epistemic uncertainty. From a practical expert panel by the Lawrence Livermore National Laboratory, the Fujita, F'-scale and it's another variant were compared and weighted as 0.6, 0.322 and 0.078 each. The IAEA report [16] compared the EF-scale, F'-scale and the F-scale and assigned weights as 0.5, 0.35 and 0.15. Note that different wind speed assignments lead to different wind speed intervals, affecting the calculation of random encounter error and direct classification error.

Regarding occurrence rates, the fitting ability of the annual occurrence of tornadoes into a function is an epistemic uncertainty source. For example, EPRI Report NP-2005 [6] proposes a Poisson method, a Bayesian-Poisson method, Polya method, Weibull method, and a Bayesian-Weibull method. The reliability of such function would increase with data, which means it should be classified as epistemic uncertainties. For rare frequency events, statistic parameters contain considerable bias due to finite sample size. Such uncertainty could be treated as aleatory uncertainty. The IAEA report [16] gives the standard error (SE) of a mean value of Poisson function with sample size N as $\sqrt{(\lambda/N)}$.

Not only wind speeds and annual counts, but other data sources such as the tornado length and width also contain uncertainty due to limited data. The NUREG/CR-4461 Rev.2 [9] pointed out that less effort has been made to quantify the uncertainties in the reported tornado velocity, lengths and widths. Based on the examination there is a lack of knowledge regarding uncertainty analysis for tornado width and length information, we will suggest a method to implement such information into a hazard analysis model.

3. METHOD

3.1. TOWLA model

Climatology differs by region. A hazard model should consider characteristics specific to the region of interest. In Japan, the occurrence of tornadoes over the sea poses challenges for collecting accurate statistics, leading to potential data incompleteness or uncertainty. Furthermore, the region of interest is confined to a narrow strip along the coastline, introducing the possibility of under- or over-sampling issues, particularly when tornadoes cross the boundary. To address these challenges, Central Research Institute of Electric Power Industry has introduced the TOrnado Wind speed hazard for Limited Area (TOWLA) model [17]. Following the standard procedure for tornado wind hazard models, this code starts from selecting data sources and a specific region of interest. The Japan Meteorological Agency (JMA) Tornado database [18] was used in this study. Two dominant regions will be defined based on observation as will be discussed in Section 4.1.

When calculating tornado counts, it is crucial to account for missing data in the database. In some models, missing data is simply ignored due to uncertainties [19]. In Japan, a notable number of ocean tornadoes are observed along the coastline. Ignoring such data may notably underestimate tornado counts. Therefore, missing

data is considered based on its properties. In the TOWLA model, F unknown data for land tornadoes and waterspouts were treated separately. Specifically, F unknown data observed on land were categorized as into F0 tornadoes. Waterspouts, on the other hand, were distributed across all intensity levels based on the frequency distribution of land tornadoes. Such procedure to take into account F unknown tornadoes also affect the analysis of tornado width and length as these data also contain missing values. To address this, a method was employed where known data was initially sorted based on tornado length for each F-scale. Subsequently, repetitive sampling was applied until width was assigned to all F-scale data. Mean and standard deviations were then calculated, assuming a lognormal distribution. The repetitive sampling after sorting data aims to maintain conservativity of the resulting hazard curve. However, this approach may lead to unphysical underestimation of the correlation factor (R). To mitigate this, the correlation factor was calculated solely using known data pairs.

Through a series of calculations, 9 characteristic parameters (U_mean, U_std, W_mean, W_std, L_mean, L_std, r_UW, r_UL, r_WL) were determined. These parameters were substituted into the expected damage area ($E(DA\ (V_0))$ model by Garson et al., (1975) [20]. This model calculates the damage area by integrating multivariate log-normal distributions of U, W, and L. The formula could be written as follows, where f is the multivariate lognormal distribution decided from the characteristic parameters:

$$E\big(DA(V_0)\big) = \int_0^\infty \int_0^\infty \int_{V_0}^\infty f(U,W,L)dUdWdL + D_0 \int_0^\infty \int_{V_0}^\infty f(U,L)dVdL + D_0 \int_0^\infty \int_{V_0}^\infty f(U,W)dVdW + D_0^2 \int_{V_0}^\infty f(U)dU \quad (1)$$

Note that each term corresponds to the expected area noted in Figure 1. D_0 is the target diameter. Based on $E(DA\ (V_0))$, the wind hazard could was calculated from the Poisson estimation as [8]:

$$P_{v_0}(D_0) = 1 - \exp\left[-v\frac{E\big(DA(V_0)\big)}{A_0}\right] \quad (2)$$

As Eq. (2) includes the effect of tornado velocity, lengths and widths in $E(DA\ (V_0))$, the uncertainty analysis for tornado properties comes down to analyzing the uncertainties of the damage area investigation from sampled data.

3.2. Uncertainty of damage area

When drawing different samples of N individuals from a population and calculating statistical measures such as mean or standard deviation, the statistics will vary with each sample taken. The SE shows the variability of the estimator. Here, we present a method to estimate SE of characteristic parameters from limited sample, then show how to estimate damage area uncertainty. Two major resampling methods are introduced to assess the SE of tornado width, length, and wind speed. The first method is the jackknife (JK) method, which uses the linearity of the sampling bias in the data to estimate the population.

Suppose there is a random sample is denoted as $X = \{x_1, x_2, x_3, \dots x_i, \dots, x_n\}$. The JK sample excluding the ith observation from the random sample is denoted as $X_{(i)}$. If the estimator derived from sample X is $\hat{\theta}$, and the estimator derived from the mean of the JK sample $X_{(i)}$ is $\hat{\theta}_{(*)}$ then, the bias corrected JK estimate will be described as follows:

$$\hat{\theta}_{jack} = \hat{\theta} - (N-1)\big(\hat{\theta}_{(*)} - \hat{\theta}\big) \quad (3)$$

The JK estimate of sample mean ($\bar{X}_{jack}$) and the standard error (SE_{jack}) will be described as follows:

$$\bar{X}_{jack} = \bar{X} - \big\{N\bar{X} - (N-1)\bar{X}_{(i)}\big\} \quad (4)$$

$$SE_{jack} = \sqrt{\frac{N-1}{N}\sum_{i=1}^{n}\left(\hat{\theta}_{(i)} - \hat{\theta}_{(*)}\right)^2} \tag{5}$$

On the contrary, in MC method, the mean, standard deviation and variance/covariance of characteristic parameters (wind speed, tornado width, and length) will be calculated to form a multivariate log-normal distribution $f(V, W, L)$. Re-sampling data will be directly obtained using random numbers. In the present case, 16000 trials were conducted against 55.25 years of original data. The mean and standard deviation of each sample represent the unbiased mean and SE.

Based on these data, the confidence interval of damage area is given by $Var\left[\log\left(\widehat{DA}\right)\right]$. $\log\left(\widehat{DA}\right)$ can be described as a function with 9 variables $Y_i = \{V_{mean}, V_{std}, W_{mean}, W_{std}, L_{mean}, L_{std}, R_{UW}, R_{UL}, R_{WL}\}$, so a linear approximation of $\log\left(\widehat{DA}\right)$ by Taylor expansion for$Y_i = \widehat{Y}_i$ yields:

$$\begin{aligned} Var\left[\log \widehat{DA}\right] &= E\left[\left(\sum_{i=1}^{9} a_i\left(Y_i - \widehat{Y}_i\right)\right)^2\right] \\ &\approx \sum_{i=1}^{9} a_i^2\, Var[Y_i] + \sum_{i=1}^{9}\sum_{j>i}^{9} 2a_i a_j Cov[Y_i, Y_j] \\ &= \sum_{i=1}^{9} a_i^2\, Var[Y_i] + \sum_{i=1}^{9}\sum_{j>i}^{9} 2R\left(Y_i, Y_j\right)\sqrt{a_i^2 Var[Y_i]}\sqrt{a_j^2 Var\left[Y_j\right]} \end{aligned} \tag{6}$$

where the correlation coefficient for each term is expressed using R and a_i, which is the slope of the partial derivative of $\log\left(\widehat{DA}\right)$ at $Y_i = \widehat{Y}_i$ with respect to the parameter of interest as follows:

$$a_i = \left(\frac{\partial \log(DA)}{\partial Y_i}\right)_{Y_i = \widehat{Y}_i} = \frac{\log\left(DA\left(Y_i + SE(Y_i)\right)\right)\log\left(DA(Y_i)\right)}{\Delta SE(Y_i)} \tag{7}$$

Note that the positive and negative SEs were handled independently, resulting in of 19 parastatal damage area analysis. The correlation coefficient could be calculated from JK and MC samples. In this study, we also refer Central Research Institute of Electric Power Industry (CRIEPI) report No. O19005 [21] and calculated theoretical value using covariance-variance matrices. Note that this method relies on the assumption that the data fulfills independent and identically distributed (IID) condition.
Using $Var\left[\log\left(\widehat{DA}\right)\right]$, the confidence interval of the hazard for and interval α is written using an inverse survival function S^{-1} as follows:

$$P_{v_0}(D_0) = 1 - \exp\left[-v\frac{1.0 \times 10^{\left(\log\left(DA(V_0)\right) \pm S^{-1}(1-\alpha)\sqrt{Var[\log \widehat{DA}]}\right)}}{A_0}\right] \tag{8}$$

4. HAZARD ANALYSIS

4.1. Analysis settings

Figure 2a presents the map of the location and intensity ratings of observed tornadoes across Japan during the F-scale era (1961–2016). Based on F-scale observations, F3 tornadoes are among the severest for tornadoes historically witnessed in Japan. These tornadoes are mostly concentrated around the southern area along the Pacific coastline region. Tornados in this region are not equally distributed, but rather seen to form concentrated groups along the plains. In contrast, the Sea of Japan coastline witnesses a significant number of F unknown and F0 tornadoes, equally distributed along the coastline. As for area from the coastline, the guideline of countermeasure for tornado to NPPs in Japan [22] pointed out that more than 70 % of the tornadoes in Japan are observed <10 km from the coastline (JMA database from 1961/1–2008/8). The number of tornadoes and waterspouts were almost equally distributed with the vicinity of coastline having the maximum

counts. To strike the balance between data numbers and regionality, we decided that selecting a region 5 km landside from the coastline should make a valid dataset for the present case. Based on such observations, tornadoes belonging to the Pacific coastline region and the Sea of Japan region were selected as shown in Figure 2b,c. Note that landfalling waterspouts were included in the analysis as tornadoes. Comparing Figure 2a and c, it may be evident that the number of tornadoes near the Sea of Japan coastline is significantly dropping compared to the map showing entire Japan. As shown in the enlarged map, this is because considerable counts of waterspouts are witnessed near the coastline region. Such an effect should be considered as a source of annual return period underestimation. However, in terms of damage area uncertainty analysis, tornado statistics of waterspouts are unavailable. Therefore, such information will not affect the discussions of the present paper.

Figure 3 further illustrates the annual tornado counts observed in Japan from 1991 to 2016. The JMA database underwent major updates in 1991 and 2007 during the F-scale era. The results indicate a significant increase in total number of tornadoes during these update years, particularly in 2007. Examining the breakdown, the number of F unknown and F0 tornadoes undergoes a notable change in 2007, while the counts of F1–F3 tornadoes do not exhibit a significant increase in 1991. However, considering older data, the counts of F1 tornadoes were notably low when recording started. Based on these observations, the data collection period for F0 and F unknown tornados were set as (Jan. 2007 – Mar. 2016), (Jan. 1991 – Mar. 2016) for F1 tornadoes and (Jan. 1961 – Mar. 2016) for F2 and beyond.

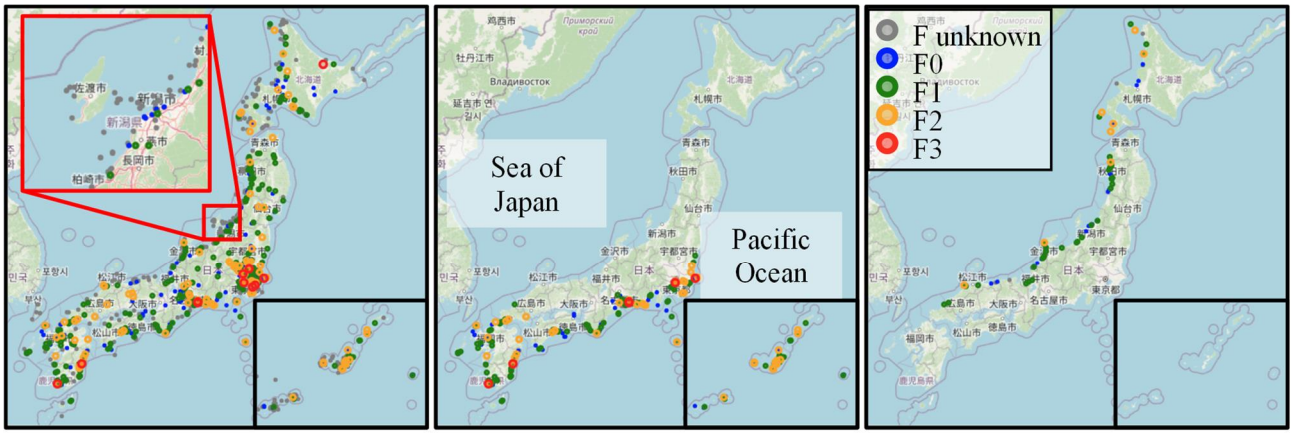

(a) Entire Japan, including ocean tornados

(b) Pacific Ocean region, 0–5 km from coastline that hit the land

(c) Sea of Japan region, 0–5 km from coastline that hit the land

Figure 2. Observed tornados in Japan (Jan. 1961 ~ Mar. 2016)

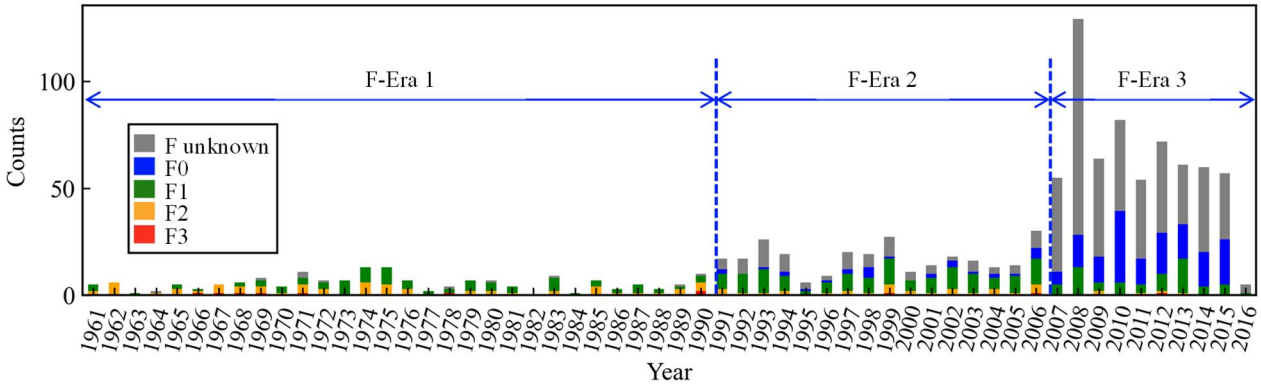

Figure 3. Tornado counts (Jan. 1961 ~ Mar. 2016)

A comparison of tornado counts for the two regions, are shown in Table 1. The observed data represent the statistics for each sub-period defined for wind categories. The pseudo data was generated by adding back the data into a full period, in this case 55.25 years. As F2–F4 tornadoes were already collected in full period, the observed and the pseudo data do not show any difference. The difference between the observed data and the pseudo data was nearly double to triple the original data. The Pacific Ocean Coastline region had almost twice

the number of tornadoes compared to the Sea of Japan region. The number of severe tornadoes had even more deviations. On the other hand, the standard deviation did not show many differences.

Table 2 shows the simulation parameters used for hazard analysis, the width and length calculated from repetitive sampling using the pseudo counts of tornadoes as explained in Section 3.1. The Pacific Ocean region had superior mean velocity and length. This is related to the fact that more severe tornadoes are observed in this area. On the other hand, the tornado width did not show much difference. As shown in correlation coefficient between velocity and width, width information tended to have less correlation against tornado intensity compared to length. It is noteworthy that correlation between width and length were significantly different between the Pacific Ocean and the Sea of Japan case. These differences address important tornado characteristics between the two regions.

Table 1. Tornado counts

Region	Type	Parameter	F0	F1	F2	F3	F4	Unknown	Total
Pacific Ocean (29614 km^2)	Observed	Counts	74	127	49	6	0	21	277
		Mean	1.34	2.30	0.89	0.11	0.00	0.38	5.01
		Std.	2.62	2.10	1.06	0.31	0.00	0.73	3.61
	Pseudo	Counts	401	195	49	6	0		651
		Mean	7.26	3.53	0.89	0.11	0.00		11.78
		Std.	3.83	2.21	1.06	0.31	0.00		4.56
Sea of Japan (14644 km^2)	Observed	Counts	38	39	10	0	0	12	99
		Mean	0.69	0.71	0.18	0.00	0.00	0.22	1.79
		Std.	2.08	0.87	0.47	0.00	0.00	0.49	2.36
	Pseudo	Counts	246	46	10	0	0		302
		Mean	4.45	0.83	0.18	0.00	0.00		5.47
		Std.	4.00	0.90	0.47	0.00	0.00		4.12

Table 2. Simulation parameters

Region	Parameter	Counts	Velocity [m/s]	Width [m]	Length [m]	Corr (U,W)	Corr (U,L)	Corr (W,L)
Pacific Ocean	Mean	11.78	33.10	121.05	2247.31	0.30	0.42	0.39
	Std.	4.56	11.74	187.98	3088.53			
Sea of Japan	Mean	5.47	28.67	121.43	1723.18	0.10	0.35	0.56
	Std.	4.12	8.29	140.63	2896.70			

4.2. Results and discussion

Using the simulation parameters outlined in Table 2, wind hazard calculations were conducted using Eqs. (1) and (2), employing two resampling methods: the MC method and the JK method. For reference, we set the target diameter as 100 m. Note that this setting is not directly related to actual power plants. When discussing the potential impact of target diameter settings on the results, it is crucial to consider that the second, third, and fourth terms of Eq. (1) are associated with the target diameter. Generally, both tornado width and target diameter are smaller than the length, implying that terms 1 and 2 will be the dominant factors. With tornado length and velocity being the dominant parameters, the Pacific Ocean region exceeds the Sea of Japan region, suggesting that the target diameter will not significantly influence their relative relationships. Although the results may underestimate the sensitivity of tornado width, as discussed in Section 4.1, width was found to be less sensitive to tornado severity. Figure 4 illustrates the resulting hazard curve, where the black plot represents the hazard curve without considering sampling bias. The black dashed plot and the red dashed hazard curve represent the hazard curve with parameters considering sampling bias using the JK and MC methods, respectively. Given that the Pacific Ocean region has more counts, higher velocity, and length, higher wind speeds were observed for the same return period in this region. Both the Pacific Ocean and the Sea of Japan region exhibit minimal influence from sampling bias. Figure 5 illustrates the mean resampling data of characteristic parameters. It's important to note that Figure 5 is a dual-axis graph, with the right axis representing the mean and standard deviation of lognormal parameters derived from U_mean, U_std, W_mean, W_std, L_mean, and L_std. The left axis represents the correlation of two parameters using logarithmic values. The values are nearly equivalent for both MC and JK methods, providing an explanation for the results observed in Figure 4.

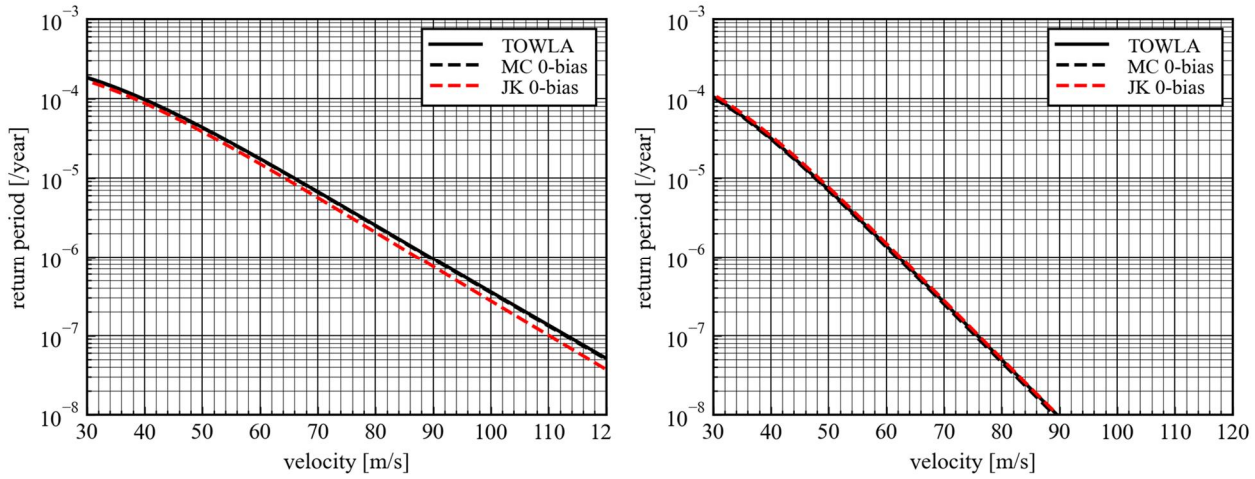

(a) Pacific Ocean region (b) Sea of Japan region

Figure 4. Comparison of hazard curves

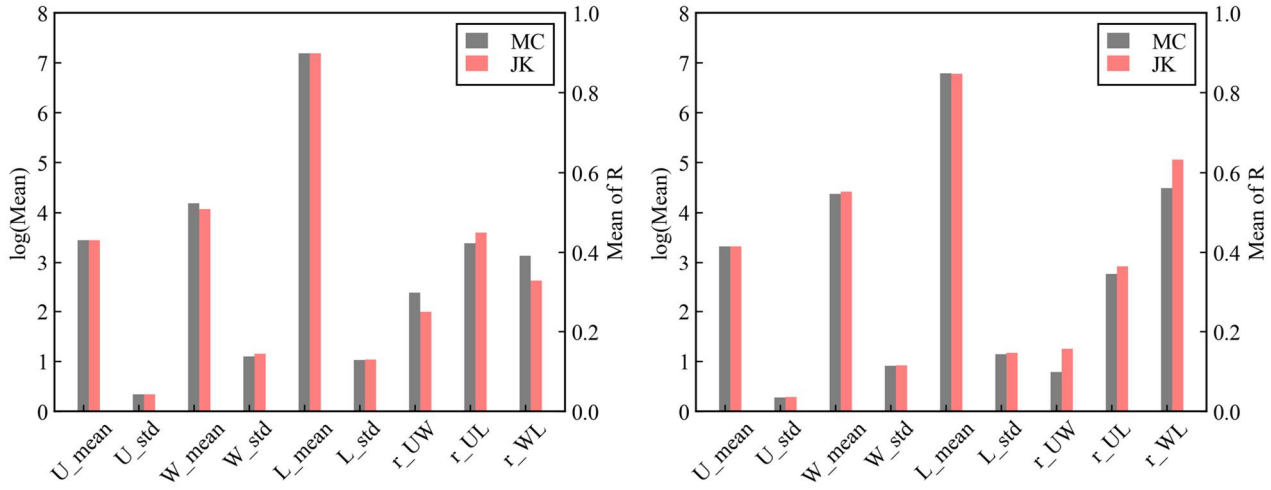

(a) Pacific Ocean region (b) Sea of Japan region

Figure 5. Comparison of sample means for 9 characteristic parameters

Based on these unbiasing methods, the 95% confidence interval was calculated using Eqs. (6) and (8). The standard error (SE) and correlation matrix needed to be determined, additionally. In the case of JK method, SE was derived from Eq. (5). In the case of MC method, the SE was obtained directly from the MC samples. Additionally, theoretical values were derived from CRIEPI report No. O19005 [21], with mean and SE values represented as $\sigma/\sqrt{N}$ and $\sigma/\sqrt{2N}$, respectively. The correlation matrix was derived from the mean of MC and JK samples for the original case, while the method outlined by CRIEPI report No. O19005 [21] was used for the theoretical case. Figure 6 presents a comparison of each method, with results compared to the original TOWLA (black solid line) and a sensitivity analysis case involving the addition of a single F3 tornado (green dashed line). The parameters of the F3 tornado were determined based on the 1999 tornado in Toyohashi city, one of the severest tornados in JMA record. Clear differences were observed between each condition. Both the MC and JK cases exhibited higher velocity for the same return period compared to their theoretical counterparts. Additionally, using the same correlation matrix, the MC case tended to exceed the JK simulation results. The effect of adding a single F3 tornado was highly sensitive in the Sea of Japan region, where adding a single event to a region that had never experienced an F3 tornado before had a noticeable impact. However, the effect was almost negligible in the Pacific Ocean region. Figure 5 illustrates the SE for each characteristic parameter outlined in Table 2. It is evident that the size of the confidence interval could be explained by the size of the SE for each condition. As explained in Section 3.1, repetitive sampling is applied when generating the pseudo data, resulting in a data degree of freedom less than the sample size, indicating that the IID assumption is not fulfilled. This means that both JK resampling and theoretical SE and correlation matrix calculation become invalid, while it has the advantage of less computational cost. The results suggest that the application of JK

and theoretical correlation may lead to underestimations of confidence intervals due to ineligible counts of unknown tornadoes.

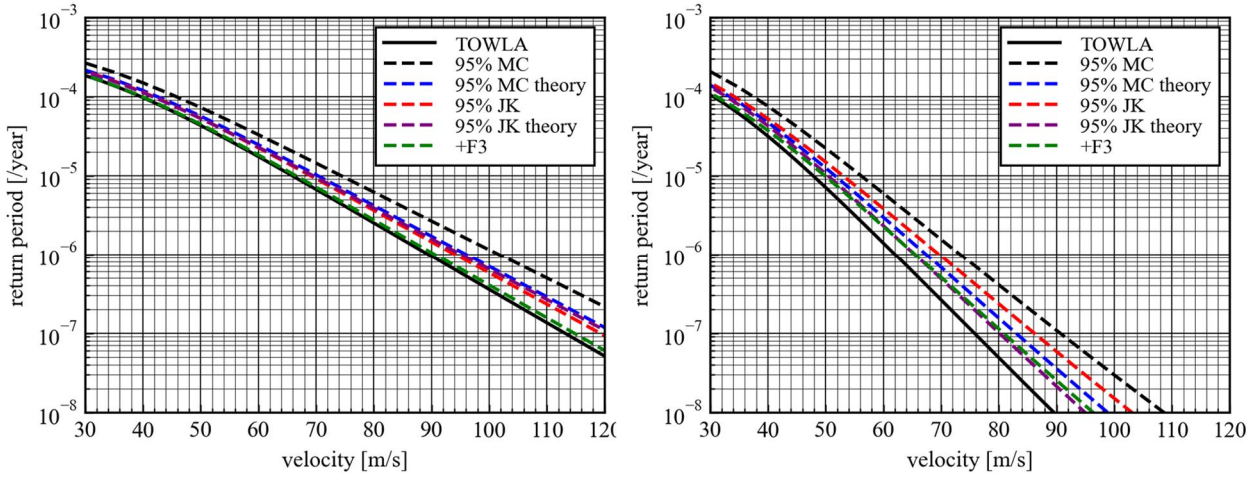

(a) Pacific Ocean region (b) Sea of Japan region

Figure 6. Comparison of hazard curve confidence intervals

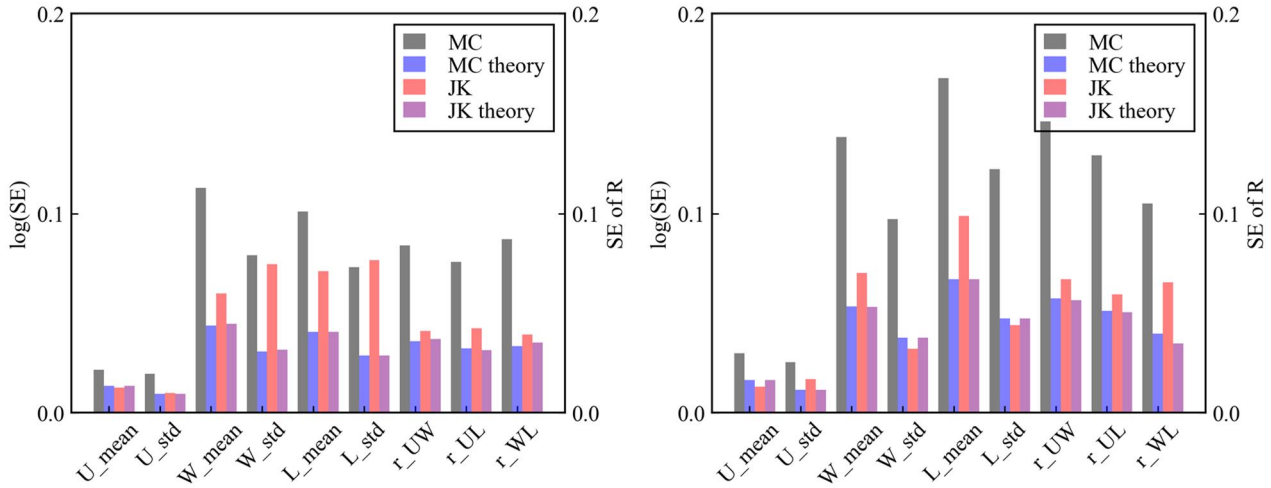

(a) Pacific Ocean region (b) Sea of Japan region

Figure 7. Comparison of sample SEs for 9 characteristic parameters

5. CONCLUSION

In this article, we have presented methodologies for considering uncertainty regarding tornado width and length as a damage area uncertainty. Two regions; the Pacific Ocean region and the Sea of Japan region was selected as characteristic area. The Pacific Ocean region was characterized by relatively powerful tornadoes concentrated in distributed plains, while the Sea of Japan region having weaker or missing tornadoes, including waterspouts wide spreading along the coastline region. Such differences in tornado characteristics impacted the hazard curve, with the Pacific Ocean region having higher wind speed for same return period. A comparative case study was conducted for hazard curves and confidence intervals at each regions using different re-sampling/SE and correlation matrix analysis methods. The 95 % confidence interval derived from the damage area uncertainty analysis was comparable or larger than adding a sole F3 tornado to the given domain. Among the methods that were compared, the Monte Carlo simulation-based method was determined to have the largest confidence interval, while also being identified as most appropriate among the compared methods. This was because repetitive sampling is applied to deal with unknown/missing tornado data, the IID assumption is not fulfilled. Such conclusion could be reinforced from the fact that this error was larger for the case in Sea of Japan region, containing a higher proportion of unknown/missing data. Since the handling of unknown/missing data is crucial when evaluating Japanese tornadoes, this underestimation due to incorrect SE

parameters is an ineligible factor. Despite the drawbacks of heavy computation, the application of Monte Carlo simulation was crucial for this kind of application.

References

[1] Rotunno R. The fluid dynamics of tornadoes. Annual Review of Fluid Mechanics, 45, pp. 59–84, 2013.
[2] Niino H, Fujitani T, and Watanabe N. A statistical study of tornadoes and waterspouts in Japan from 1961 to 1993. Journal of Climate, 10(7), pp. 1730–1752, 1997.
[3] Prevatt D O, Agdas D, Thompson A, Tamura Y, Matsui M, and Okada R. Tornado Damage and Impacts on Nuclear Facilities in the United States. Journal of Wind Engineering, 40(3), pp. 91–100, 2015.
[4] USNRC. Design-basis tornado and tornado missiles for nuclear power plants, Regulatory Guide 1.76, 2007.
[5] Inoue H, Fukunishi S, and Suzuki T. Assessment guide for tornado effect on Nuclear Power Plants (draft) with its commentaries, JNES-RE–2013-9009 (in Japanese), 2013.
[6] Twisdale L A, and Dunn W L. Tornado Missile Simulation and Design Methodology, Volume 2: Model Verification and Database Updates (NP-2005-V2), 1981.
[7] Twisdale L A, Dunn W L, and Chu J. Tornado Missile Risk Analysis: Tornado missile risk analysis: probability modeling, simulation methodology, and case studies. Final report (NP-768). EPRI, 1978.
[8] Twisdale L A, Dunn W L, Lew S T, Davis T L, Hsu J C, and Lee S T. Tornado missile risk analysis. Appendixes: analytical models and data bases. Final report (NP-769), 1978.
[9] Ramsdell J V, and Rishel J J P. Tornado Climatology of the Contiguous United States. Pacific Northwest National Laboratory (NUREG/CR-4461 Rev. 2), 2007.
[10] ASME/ANS. Addenda to ASME/ANS RAS– 2008 Standard for Level 1/Large Early Release Frequency Probabilistic Risk Assessment for Nuclear Power Plant Applications, 2013.
[11] Reinhold T A, and Ellingwood B. Tornado damage risk assessment (NUREG/CR-2944), 1982.
[12] Faletra K, Twisdale L A, and Banik S S. Probabilistic modelling of tornado path length intensity variation using F/EF-scale damage. 28th Conference on Severe Local Storms, 2016.
[13] Agee E, and Childs S. Adjustments in tornado counts, F-scale intensity, and path width for assessing significant tornado destruction. Journal of Applied Meteorology and Climatology, 53(6), pp. 1494–1505, 2014.
[14] Anderson C J, Wikle C K, Zhou Q, and Royle J A. Population Influences on Tornado Reports in the United States. Weather and Forecasting, 22(3), pp. 571–579, 2007.
[15] Tamura Y, Niino H, Ito M, Kikitsu H, Maeda J, Okuda Y, Sakata H, Shoji Y, Suzuki S, and Tanaka Y. Development and Implementation of Japanese Enhanced Fujita Scale. 28th Conference on Severe Local Storms, 2016.
[16] Safety report series No. 120. Assessment of high wind and external flooding (excluding tsunami) hazards in site evaluation for nuclear installations, 2024.
[17] Hirakuchi H, Nohara D, Sugimoto S, Eguchi Y, and Hattori Y. Development of a tornado wind speed hazard model for limited area (TOWLA) for nuclear power plants at a coastline. Central Research Institute of Electric Power Industry, Nuclear Risk Research Center Rep. O15005 (in Japanese), 2015.
[18] Japan Metrological Agency. Tornado database. https://www.data.jma.go.jp/obd/stats/data/bosai/tornado/kaisetsu/jefscale_en.html, 2023.
[19] Electric Power Research Institute. High Wind Risk Assessment Guidelines, 2015.
[20] Garson R C, Catalán J M, and Cornell C A. Tornado Design Winds Based on Risk. Journal of the Structural Division, 101(9), pp. 1883–1897, 1975.
[21] Hirakuchi H, Nohara D, Sugimoto S, Eguchi Y, and Hattori Y. Estimation method of statistical confidence limits of tornado wind hazard curves. Central Research Institute of Electric Power Industry, Nuclear Risk Research Center Rep. O19005 (in Japanese), 2020.
[22] Nuclear Regulation Authority. The guideline of countermeasure for tornado to nuclear power plants in Japan (in Japanese), 2013.